Available online at www.sciencedirect.com
SCIENCE DIRECT®
Journal of Solid State Chemistry 177 (2004) 2675–2684
JOURNAL OF SOLID STATE CHEMISTRY
http://elsevier.com/locate/jssc

Structures and syntheses of layered and framework amine-bearing uranyl phosphate and uranyl arsenates

Andrew J. Locock* and Peter C. Burns

Department of Civil Engineering and Geological Sciences, University of Notre Dame, 156 Fitzpatrick Hall, Notre Dame, IN 46556-0767, USA

Received 27 February 2004; received in revised form 22 March 2004; accepted 28 March 2004

Abstract

Two hydrated uranyl arsenates and a uranyl phosphate were synthesized by hydrothermal methods in the presence of amine structure-directing agents and their structures determined: $(N_2C_6H_{14})[(UO_2)(AsO_4)]_2(H_2O)_3$, *DabcoUAs*, $\{NH(C_2H_5)_3\}[(UO_2)_2(AsO_4)(AsO_3OH)]$, *TriethUAs*, and $(N_2C_4H_{12})(UO_2)[(UO_2)(PO_4)]_4(H_2O)_2$, *PiperUP*. Intensity data were collected at room temperature using Mo$K\alpha$ X-radiation and a CCD-based area detector. The crystal structures were refined by full-matrix least-squares techniques on the basis of F^2 to agreement indices (*DabcoUAs*, *TriethUAs*, *PiperUP*) w$R_2 = 5.6\%$, 8.3%, 7.2% for all data, and $R_1 = 2.9\%$, 3.3%, 4.0%, calculated for 1777, 5822, 9119 unique observed reflections ($|F_o| \geqslant 4\sigma_F$), respectively. *DabcoUAs* is monoclinic, space group $C2/m$, $Z = 2$, $a = 18.581(1)$, $b = 7.1897(4)$, $c = 7.1909(4)$ Å, $\beta = 102.886(1)^\circ$, $V = 936.43(9)$ Å^3, $D_{calc} = 3.50$ g/cm^3. *TriethUAs* is monoclinic, space group $P2_1/n$, $Z = 4$, $a = 9.6359(4)$, $b = 18.4678(7)$, $c = 10.0708(4)$ Å, $\beta = 92.282(1)^\circ$, $V = 1790.7(1)$ Å^3, $D_{calc} = 3.41$ g/cm^3. *PiperUP* is monoclinic, space group Pn, $Z = 2$, $a = 9.3278(4)$, $b = 15.5529(7)$, $c = 9.6474(5)$ Å, $\beta = 93.266(1)^\circ$, $V = 1397.3(1)$ Å^3, $D_{calc} = 4.41$ g/cm^3. The structure of *DabcoUAs* contains the autunite-type sheet formed by the sharing of vertices between uranyl square bipyramids and arsenate tetrahedra. The triethylenediammonium cations are located in the interlayer along with two H_2O groups and are disordered. Both *TriethUAs* and *PiperUP* contain sheets formed of uranyl pentagonal bipyramids and tetrahedra (arsenate and phosphate, respectively) with the uranophane sheet-anion topology. In *TriethUAs*, triethlyammonium cations are located in the interlayer. In *PiperUP*, the sheets are connected by a uranyl pentagonal bipyramid that shares corners with phosphate tetrahedra of adjacent sheets, resulting in a framework with piperazinium cations and H_2O groups in the cavities of the structure.

Keywords: Uranyl arsenate; Uranyl phosphate; Intercalation; Framework; Mixed organic–inorganic; Crystal structure refinement; Hydrothermal synthesis

1. Introduction

The crystal chemistry of hexavalent uranium is rich in diversity because of the high coordination numbers (six, seven, or eight) accessible to U^{6+} and the polarized distribution of bond strengths within uranyl polyhedra [1]. Polymerization of uranyl bipyramidal polyhedra generally occurs only through the equatorial ligands, usually yielding infinite chains or sheets, with three-dimensional framework structures occasionally being facilitated by linkages through non-uranyl polyhedra such as silicate [2–4], molybdate [5,6], vanadate [7], or phosphate [8,9].

The addition of organic components to form mixed organic–inorganic uranyl compounds considerably increases the potential structural variability, and such structures have been the focus of considerable research in recent years [10–28]. In the organic–uranyl–phosphate system, the use of simple amines as structure-directing agents has produced layered and framework structures [8,16] that contain uranyl phosphate sheets based on the uranophane sheet-anion topology [1]. Uranyl phosphate crown ether compounds [17] contain one-dimensional chains of uranyl pentagonal bipyramids and phosphate tetrahedra that are identical topologically to those found in simple inorganic uranyl phosphate and uranyl arsenate structures [29,30]. Extension of the system to phosphonate and its derivatives adds to the structural diversity, producing

*Corresponding author. Fax: 219-247-1206.
E-mail addresses: alocock@nd.edu (A.J. Locock), pburns@nd.edu (P.C. Burns).

0022-4596/$ - see front matter © 2004 Elsevier Inc. All rights reserved.
doi:10.1016/j.jssc.2004.03.045

chains, sheets, frameworks and even uranyl phosphonate tubes. The uranyl phosphonate chains are based either on uranyl square bipyramids [18,19] and are similar to the uranyl arsenate chains of the walpurgite group minerals [31,32], or are based on uranyl pentagonal bipyramids [20] and are similar to those chains found in the crown ether compounds and simple uranyl phosphate and uranyl arsenate compounds [17,26,27]. Sheet structures based on the uranophane sheet-anion topology [1] are known from uranyl phosphonates [18,21], as are tube structures [22–25], but new sheet and framework topologies as yet undiscovered in inorganic uranyl phosphate or uranyl arsenate systems have also been crystallized in uranyl phosphonates [26]. In addition to the framework structures formed in the phosphate- and phosphonate-based systems, novel microporous solids have been synthesized in the organic–uranyl–phosphite and organic–uranyl–phosphate–fluoride systems [27,28].

We are interested in extending our understanding of the rich solid-state chemistry of uranium, and to this end, have undertaken the hydrothermal synthesis of uranyl arsenates and uranyl phosphates in the presence of amine structure-directing agents, and report their crystal structures herein.

2. Experiment

2.1. Crystal synthesis

Single crystals of $(N_2C_6H_{14})[(UO_2)(AsO_4)]_2(H_2O)_3$, *DabcoUAs*, $\{NH(C_2H_5)_3\}[(UO_2)_2(AsO_4)(AsO_3OH)]$, *TriethUAs*, and $(N_2C_4H_{12})(UO_2)[(UO_2)(PO_4)]_4(H_2O)_2$, *PiperUP*, were obtained by hydrothermal reaction. Uranyl acetate, $UO_2(CH_3COO)_2(H_2O)_2$ (98%, Alfa Aesar), triethylenediamine, $N_2C_6H_{12}$ (1,4-diazabicyclo[2.2.2]octane, DABCO, 98%, Aldrich), triethylamine, $N(C_2H_5)_3$ (99%, Aldrich), concentrated HCl (37.2%, Fisher), and natural fluorapatite, $Ca_5(PO_4)_3F$ (Liscombe Deposit, near Wilberforce, Ontario, Canada) were used as received. Hydrogen arsenate, $H_5As_3O_{10}$, was prepared from As_2O_3 (99%, Aldrich) and concentrated HNO_3 (69.2%, Fisher) by the method of Walton [33]. Millepore-filtered ultrapure water (18 MΩ resistance) was used in all reactions. Reactions were carried out in 23 mL polytetrafluoroethylene-lined Parr acid-reaction vessels. Reaction yields were not quantitatively determined.

2.1.1. $(N_2C_6H_{14})[(UO_2)(AsO_4)]_2(H_2O)_3$

DabcoUAs, was synthesized by hydrothermal reaction of $UO_2(CH_3COO)_2(H_2O)_2$ (124.0 mg, 0.294 mmol), $N_2C_6H_{12}$ (109.6 mg, 0.972 mmol), $H_5As_3O_{10}$ (153.7 mg, 0.394 mmol), concentrated HCl (0.334 g, 3.406 mmol) and ultrapure H_2O (6107 mg). The mixture was heated at 190(1)°C in a Fisher Isotemp oven for 3 days. The autoclave was then removed to air and allowed to cool to room temperature.

2.1.2. $\{NH(C_2H_5)_3\}[(UO_2)_2(AsO_4)(AsO_3OH)]$

TriethUAs was synthesized by hydrothermal reaction of $UO_2(CH_3COO)_2(H_2O)_2$ (111.1 mg, 0.262 mmol), $N(C_2H_5)_3$ (144.8 mg, 1.431 mmol), $H_5As_3O_{10}$ (116.0 mg, 0.298 mmol), concentrated HCl (0.1445 g, 1.474 mmol) and ultrapure H_2O (4132 mg). The mixture was heated at 6° per hour from 60°C to 220(1)°C, held at 220(1)°C for 24 h and cooled to 90(1)°C at 6° per hour. The autoclave was then removed to air and allowed to cool to room temperature.

2.1.3. $(N_2C_4H_{12})(UO_2)[(UO_2)(PO_4)]_4(H_2O)_2$

PiperUP, was synthesized by hydrothermal reaction of $UO_2(CH_3COO)_2(H_2O)_2$ (99.9 mg, 0.236 mmol), $N_2C_6H_{12}$ (11.8 mg, 0.105 mmol), $Ca_5(PO_4)_3F$ (105.7 mg, 0.210 mmol), concentrated HCl (0.1858 g, 1.896 mmol) and ultrapure H_2O (4074 mg). The mixture was heated at 190(1)°C in a Fisher Isotemp oven for 3 days. The autoclave was then removed to air and allowed to cool to room temperature. Interestingly, the product of this reaction contains the piperazinium cation $(N_2C_4H_{12})^{2+}$, rather than the triethylenediammonium cation $(N_2C_6H_{14})^{2+}$. The breakdown of triethylenediamine under these reaction conditions is not entirely unexpected. In aqueous solution at room temperature, chlorine dioxide can produce piperazine from triethylenediamine by oxidative fragmentation [34]. The decomposition of triethylenediamine under hydrothermal conditions to produce the ammonium cation has also been observed in the DABCO–U–F system [14].

2.2. Single-crystal X-ray diffraction data collection

For each of the three samples, a suitable crystal was mounted on a Bruker PLATFORM three-circle X-ray diffractometer operated at 50 keV and 40 mA, and equipped with a 4 K APEX CCD detector and a crystal to detector distance of ~4.7 cm. Data were collected at room temperature using graphite-monochromatized Mo$K\alpha$ X-radiation and frame widths of 0.3° in ω. Comparison of the intensities of equivalent reflections measured at different times during data collection showed no significant decay for any of the three compounds. Selected data collection parameters and crystallographic data are provided in Table 1. SMART software [35] was used for data collection, SAINT [36] for data integration, and corrections for absorption were made with the program XPREP [37].

Systematic absences of reflections for *DabcoUAs* were consistent with space groups $C2/m$, $C2$ and Cm; the best solution was obtained in $C2/m$. In the case of *TriethUAs*, systematic absences of reflections were consistent with space group $P2_1/n$. Systematic absences

Table 1
Crystallographic data and details of the structure refinements

Compound	*DabcoUAs*	*TriethUAs*	*PiperUP*
a (Å)	18.581(1)	9.6359(4)	9.3278(4)
b (Å)	7.1897(4)	18.4678(7)	15.5529(7)
c (Å)	7.1909(4)	10.0708(4)	9.6474(5)
β (deg)	102.886(1)	92.282(1)	93.266(1)
V (Å^3)	936.43(9)	1790.7(1)	1397.3(1)
Space group	$C2/m$	$P2_1/n$	Pn
Z	2	4	2
Formula	$(N_2C_6H_{14})[(UO_2)(AsO_4)]_2(H_2O)_3$	$\{NH(C_2H_5)_3\}[(UO_2)_2(AsO_4)(AsO_3OH)]$	$(N_2C_4H_{12})(UO_2)[(UO_2)(PO_4)]_4(H_2O)_2$
Formula weight	986.128	921.099	1854.206
$F(000)$	880	1620	1596
μ (mm^{-1})	20.86	21.79	29.22
D_{calc} (g/mL)	3.497	3.413	4.407
Crystal size (mm)	$0.20 \times 0.10 \times 0.02$	$0.50 \times 0.08 \times 0.08$	$0.20 \times 0.20 \times 0.02$
Color and habit	Yellow plate	Yellow needle	yellow plate
Temperature (K)	293(2)	293(2)	293(20)
Width (deg), time(s)	0.3, 20	0.3, 10	0.3, 7
Collection (h)	Sphere, 16	Sphere, 8	sphere, 6
θ range	2.9–34.5°	2.0–34.5°	2.5–34.5°
Data collected	$h\pm29$, $k\pm11$, $l\pm11$	$h\pm15$, $k\pm29$, $l\pm15$	$h\pm14$, $k\pm24$, $l\pm15$
Absorption[a]	plate (100) 0.5°	Ellipsoid	plate (010) 3°
Total refl.	9541	36364	25986
Unique refl., R_{int}	2087, 0.088	7446, 0.088	11271, 0.061
Unique $\|F_o\|>4\sigma_F$	1777	5822	9119
Parameters	85	194	358
R_1 for $\|F_o\|>4\sigma_F$	2.9	3.3	4.0
R_1 all data, wR_2	3.6, 5.6	4.2, 8.3	4.9, 7.2
Weighting a	0.0	0.0427	0.0145
Goodness of fit	0.873	0.970	0.878
Mean shift/esd	0.000	0.000	0.000
Peaks (e/Å^3)	3.2, −1.0	5.0, −2.7	2.6, −3.2

$R_1 = [\sum||F_o| - |F_c||]/\sum|F_o| \times 100$. w$R_2 = [\sum[w(F_o^2 - F_c^2)^2]/\sum[w(F_o^2)^2]]^{0.5} \times 100$, $w = 1/(\sigma^2(F_o^2) + (aP)^2$, and $P = 1/3\max(0, F_o^2) + 2/3F_c^2$.
[a] Corrections for absorption are semi-empirical (crystal modeled either as an ellipsoid, or as a plate rejecting data within X° of the primary X-ray beam).

of reflections for *PiperUP* were consistent with space groups $P2_1/n$, $P2_1$, $P2/n$, and Pn; trial solutions were obtained in all four space groups, but the best solution was obtained in Pn. The unit cells of *TriethUAs* and *PiperUP* can be transformed to the conventional setting with space groups $P2_1/c$ and Pc, respectively, by the matrix [100/010/−101]; however, the resultant cells are quite oblique (β 134.93° and 135.72°, respectively) and therefore these structures were refined in the setting with β closer to 90°. Scattering curves for neutral atoms, together with anomalous dispersion corrections, were taken from *International Tables for* X-ray *Crystallography*, *Vol. C* [38]. The SHELXTL Version 5 series of programs [39] was used for the solution and refinement of the crystal structures.

3. Structure solution and refinement

All three structures were refined on the basis of F^2 for all unique data. In the final cycle of each refinement, the mean parameter shift/esd was 0.000.

The structure of *DabcoUAs* was solved in space group $C2/m$ using direct methods. A structure model including anisotropic displacement parameters for all non-H atoms converged, and gave an agreement index (R_1) of 2.9%, calculated for the 1771 observed unique reflections ($|F_o| \geqslant 4\sigma_F$). The locations of the H atoms in the unit cell were not determined.

The structure of *TriethUAs* was solved in space group $P2_1/n$ using Patterson methods. A structure model including anisotropic displacement parameters for U, As, N and O atoms converged, and gave an agreement index (R_1) of 3.3%, calculated for the 5822 observed unique reflections ($|F_o| \geqslant 4\sigma_F$). Possible H atom positions around N(1) and O(12) were located in difference-Fourier maps, calculated following refinement of the model. Their positions were refined with the restraint that O–H bond-lengths be ~0.96 Å and with fixed isotropic displacement parameters.

The structure of *PiperUP* was solved in space group Pn using direct methods. A structure model including the racemic twin law [−100/0−10/00−1] and anisotropic displacement parameters for U, P and fully occupied O atoms converged, and gave an agreement index (R_1) of

4.0%, calculated for the 9119 observed unique reflections ($|F_o| \geq 4\sigma_F$). The racemic twin-component scale factor refined to 0.491(7), consistent with an even distribution of the enantiomorphic components. The locations of the H atoms in the unit cell were not determined. The refined solution obtained for *PiperUP* was checked with the ADDSYM algorithm in the program PLATON [40,41] but no higher symmetry was found. The arrangement of the U atoms in *PiperUP* is consistent with a non-centrosymmetric structure; upon testing the *Pn* model with only isotropic U atoms present, the ADDSYM algorithm does not reveal any higher symmetry, and solutions by direct or Patterson methods of *PiperUP* in space groups $P2_1/n$, $P2_1$ and $P2/n$ yield U positions with displacement parameters and interatomic distances that are physically unrealistic.

The atomic positional parameters and displacement parameters of the three compounds are given in Table 2—*DabcoUAs*, Table 3—*TriethUAs*, and Table 4—*PiperUP*. Selected interatomic distances are listed in Table 5—*DabcoUAs*, Table 6—*TriethUAs* and Table 7—*PiperUP*.

4. Results

4.1. Structure description

DabcoUAs contains the well-known corrugated autunite-type sheet formed by the sharing of vertices between uranyl square bipyramids and arsenate tetrahedra (Fig. 1), with composition $[(UO_2)(AsO_4)]^-$, which was originally described by Beintema [42]. The triethylenediammonium cations are located in the interlayer region between the uranyl arsenate sheets (Fig. 2), along with two symmetrically independent H_2O groups that are held in the structure only by hydrogen bonding. Most of the interlayer contents in *DabcoUAs* are disordered, with the pseudo-trigonal triethylenediammonium cation occupying either of two orientations in competition with an H_2O group (Fig. 3). Thus, N(1A), C(2A), and OW(2A) are half occupied, and N(1A) is separated from its symmetry equivalent by 1.39(2) Å, whereas OW(2A) is separated from C(2A) by 1.27(1) Å. The local environment is displayed in Fig. 4: the triethylenediammonium cation is separated locally from OW(2A) by 3.4–3.5 Å. The disorder present in the $C2/m$ model for *DabcoUAs* prompted a search for a larger unit cell in accord with the cautions of Marsh [43]. The intensity data were examined carefully, but no significant indications of a larger cell were found, despite the high sensitivity of the CCD detector [44].

TriethUAs is isostructural with its phosphate analogue, $\{NH(C_2H_5)_3\}[(UO_2)_2(PO_4)(PO_3OH)]$, [16], CSD collection code NECPEQ, space group $P2_1/n$. These compounds contain uranyl arsenate and uranyl phosphate sheets, respectively, that are topologically

Table 2
Atomic coordinates ($\times 10^4$) and displacement parameters ($Å^2 \times 10^3$) for *DabcoUAs*, $(N_2C_6H_{14})[(UO_2)(AsO_4)]_2(H_2O)_3$

	x	*y*	*z*	U_{eq}
U(1)	3042(1)	5000	−2158(1)	12(1)
As(1)	2510(1)	5000	2514(1)	15(1)
O(1)	3099(3)	5000	1049(6)	22(1)
O(2)	4041(3)	5000	−1571(7)	23(1)
O(3)	3055(3)	5000	4706(6)	26(1)
O(4)	2063(3)	5000	−2655(7)	30(1)
O(5)	1953(2)	3144(4)	2129(5)	26(1)
OW(1)	409(4)	0	7111(9)	65(2)
OW(2A)	699(8)	5000	−601(19)	61(4)
N(1A)	157(5)	3252(12)	5975(12)	29(2)
C(1)	612(3)	3944(7)	−5416(8)	31(1)
C(2A)	530(7)	3935(16)	7967(15)	35(3)

Note: U_{eq} is defined as one-third of the trace of the orthogonalized U_{ij} tensor.
OW(2A), N(1A) and C(2A) are half occupied. N(1A) is separated from its symmetry equivalent by 1.39(2) Å. OW(2A) is separated from C(2A) by 1.27(1) Å.

Table 3
Atomic coordinates ($\times 10^4$) and displacement parameters ($Å^2 \times 10^3$) for *TriethUAs*, $\{NH(C_2H_5)_3\}[(UO_2)_2(AsO_4)(AsO_3OH)]$

	x	*y*	*z*	U_{eq}
U(1)	801(1)	2325(1)	810(1)	14(1)
U(2)	−228(1)	2340(1)	4679(1)	13(1)
As(1)	−1681(1)	2850(1)	−1939(1)	15(1)
As(2)	−2774(1)	2172(1)	2437(1)	13(1)
O(1)	−3552(3)	2741(2)	1361(3)	20(1)
O(2)	−2714(3)	2530(2)	4007(3)	20(1)
O(3)	−3405(3)	2895(2)	−1763(3)	23(1)
O(4)	−1025(3)	2148(2)	2261(3)	20(1)
O(5)	−851(3)	2301(2)	−891(4)	26(1)
O(6)	−1692(3)	2550(2)	−3522(3)	21(1)
O(7)	1000(3)	1376(2)	654(3)	23(1)
O(8)	−3510(3)	1364(2)	2426(3)	24(1)
O(9)	−511(4)	1401(2)	4841(3)	24(1)
O(10)	618(4)	3267(2)	1003(4)	27(1)
O(11)	47(4)	3273(2)	4474(4)	26(1)
O(12)	−1035(4)	3700(2)	−1863(4)	31(1)
N(1)	−2354(6)	−8(3)	2521(6)	49(2)
C(1)	−831(9)	145(5)	2375(8)	59(2)
C(2)	−49(9)	538(6)	7751(8)	65(2)
C(3)	−1953(9)	4582(5)	3611(9)	69(2)
C(4)	−1982(12)	5005(7)	4873(12)	94(3)
C(5A)	−2290(20)	−318(12)	3918(13)	82(6)
C(5B)	−2885(17)	−433(8)	3681(13)	50(4)
C(6A)	−3580(20)	−11(12)	4600(20)	88(6)
C(6B)	−2550(20)	−6(10)	4977(19)	66(4)
H(1)	−40(20)	3710(40)	−1850(70)	50[a]
H(2)	−2780(60)	476(19)	2410(60)	50[a]

Note: U_{eq} is defined as one-third of the trace of the orthogonalized U_{ij} tensor.
C(5A), C(5B), C(6A) and C(6B) are half occupied. C(5A) is separated from C(5B) by 0.65(2) Å. C(6A) is separated from C(6B) by 1.05(3) Å.
[a] Value constrained during refinement.

Table 4
Atomic coordinates ($\times 10^4$) and displacement parameters ($Å^2 \times 10^3$) for *PiperUP*, $(N_2C_4H_{12})(UO_2)[(UO_2)(PO_4)]_4(H_2O)_2$

	x	y	z	U_{eq}
U(1)	1420(1)	170(1)	290(1)	15(1)
U(2)	2385(1)	228(1)	−3651(1)	14(1)
U(3)	1337(1)	4892(1)	13(1)	15(1)
U(4)	2285(1)	4707(1)	−3945(1)	14(1)
U(5)	2166(1)	7488(1)	3112(1)	16(1)
P(1)	4800(3)	4369(2)	−1617(2)	13(1)
P(2)	−1214(3)	4739(2)	−2250(3)	13(1)
P(3)	4888(3)	638(2)	−1378(3)	12(1)
P(4)	−1136(3)	300(2)	−2008(2)	13(1)
O(1)	3242(8)	563(6)	−1220(8)	14(2)
O(2)	497(8)	425(6)	−2165(8)	20(2)
O(3)	401(9)	4606(6)	−2448(9)	23(2)
O(4)	3140(8)	4445(6)	−1463(8)	15(2)
O(5)	1799(8)	5948(6)	−417(8)	22(2)
O(6)	1823(8)	−896(5)	−125(9)	21(2)
O(7)	4886(8)	4606(5)	−3185(8)	20(2)
O(8)	5579(8)	5047(5)	−720(8)	18(2)
O(9)	−1849(8)	5393(5)	−3350(8)	17(2)
O(10)	−1190(7)	5175(5)	−798(7)	19(2)
O(11)	−1760(9)	−397(6)	−3014(9)	23(2)
O(12)	2372(8)	5806(6)	−3603(9)	27(2)
O(13)	2452(9)	−880(6)	−3302(9)	31(2)
O(14)	817(7)	3828(6)	349(8)	23(2)
O(15)	5673(8)	8(6)	−431(8)	21(2)
O(16)	2160(8)	3600(5)	−4240(8)	26(2)
O(17)	974(8)	1237(6)	663(8)	25(2)
O(18)	−2030(8)	3914(6)	−2311(8)	26(2)
O(19)	−1110(8)	−70(6)	−507(7)	22(2)
O(20)	−1934(8)	1126(5)	−2171(8)	26(2)
O(21)	4985(8)	327(5)	−2895(7)	20(2)
O(22)	2329(9)	1328(5)	−3961(8)	28(2)
O(23)	5293(7)	3474(5)	−1319(7)	18(2)
O(24)	5374(7)	1538(5)	−1165(7)	21(2)
O(25)	2850(8)	7455(6)	4854(9)	32(2)
O(26)	1475(8)	7518(6)	1388(8)	27(2)
O(27)	4728(11)	7484(7)	2317(14)	73(4)
N(1)	417(18)	7718(12)	−1950(17)	89(5)
N(2)	2527(15)	2718(9)	2191(14)	64(4)
C(1)	−705(16)	7591(11)	−958(15)	47(4)
C(2)	3531(18)	2572(14)	1100(20)	80(6)
C(3)	2884(16)	2150(11)	−6592(15)	52(4)
C(4)	5041(17)	2750(14)	1801(18)	73(5)
OW(1)	4280(40)	7310(30)	7750(40)	145(14)
OW(2)	−180(30)	1920(20)	−5450(30)	112(10)

Note: U_{eq} is defined as one-third of the trace of the orthogonalized U_{ij} tensor.
OW(1) and OW(2) are half occupied and separated from each other by 2.15(5) Å.

Table 5
Selected interatomic distances (Å) and angles (deg) for *DabcoUAs*

U(1)–O(4)	1.774(5)	As(1)–O(3)	1.672(5)
U(1)–O(2)	1.809(5)	As(1)–O(5)	1.674(3)
U(1)–O(5)	2.260(3)	As(1)–O(5)[b]	1.673(3)
U(1)–O(5)[a]	2.260(3)	As(1)–O(1)	1.680(4)
U(1)–O(3)	2.261(4)	⟨As(1)–O⟩	1.675
U(1)–O(1)	2.285(4)		
⟨U(1)–O_{ap}⟩	1.79	N(1A)–C(1)	1.48(1)
⟨U(1)–O_{eq}⟩	2.27	N(1A)–C(2A)	1.53(1)
O(4)–U(1)–O(2)	178.2(2)	N(1A)–C(1)[c]	1.53(1)
		C(1)–C(1)[b]	1.52(1)
OW(1)–N(1A)	2.486(9)	C(2A)–C(2A)[b]	1.53(2)
OW(1)–N(1A)[d]	2.486(9)		
OW(1)–O(1)	2.793(8)	OW(2A)–N(1A)	2.748(15)
OW(1)–C(2A)	2.89(1)	OW(2A)–N(1A)[e]	2.748(15)

Symmetry transformations used to generate equivalent atoms: a: $x+1/2, -y+1/2, -z$; b: $x, -y+1, z$; c: $x, y, z+1$; d: $x, -y, z$; e: $x, -y+1, z-1$.

Table 6
Selected interatomic distances (Å) and angles (deg) for *TriethUAs*

U(1)–O(10)	1.760(4)	As(1)–O(5)	1.647(4)
U(1)–O(7)	1.771(3)	As(1)–O(3)	1.680(3)
U(1)–O(5)	2.292(4)	As(1)–O(6)	1.687(3)
U(1)–O(4)	2.354(3)	As(1)–O(12)	1.691(4)
U(1)–O(2)	2.372(3)	⟨As(1)–O⟩	1.68
U(1)–O(6)	2.493(3)		
U(1)–O(3)	2.564(3)	As(2)–O(8)	1.651(3)
⟨U(1)–O_{ap}⟩	1.765	As(2)–O(1)	1.666(3)
⟨U(1)–O_{eq}⟩	2.42	As(2)–O(4)	1.702(3)
O(10)–U(1)–O(7)	178.7(2)	As(2)–O(2)	1.712(3)
		⟨As(2)–O⟩	1.68
U(2)–O(11)	1.756(4)		
U(2)–O(9)	1.764(3)	N(1)–C(3)	1.50(1)
U(2)–O(1)	2.298(3)	N(1)–C(1)	1.51(1)
U(2)–O(3)	2.363(3)	N(1)–C(5B)	1.514(8)
U(2)–O(6)	2.372(3)	N(1)–C(5A)	1.517(9)
U(2)–O(2)	2.488(3)		
U(2)–O(4)	2.549(3)	N(1)–H(2)	0.99(2)
⟨U(2)–O_{ap}⟩	1.76	H(2)···O(8)	1.79(2)
⟨U(2)–O_{eq}⟩	2.41	N(1)–H(2)···O(8)	173
O(11)–U(2)–O(9)	178.6(2)		
		C(1)–C(2)	1.53(1)
O(12)–H(1)	0.95(2)	C(3)–C(4)	1.49(1)
H(1)···O(8)	1.68(2)	C(5A)–C(6A)	1.55(3)
O(12)–H(1)···O(8)	153	C(5B)–C(6B)	1.55(3)

D–H···A angles rounded to the nearest degree.

identical to the uranyl silicate sheets in uranophane-beta, $Ca[(UO_2)SiO_3OH)]_2(H_2O)_5$ [45]. There are two symmetrically independent U atoms in *TriethUAs*, each of which is part of an approximately linear $(UO_2)^{2+}$ cation. The uranyl ions are coordinated by five additional ligands arranged at the equatorial positions of pentagonal bipyramids, with the uranyl O atoms at the apices of the bipyramids. The U(1) and U(2) pentagonal bipyramids share an equatorial edge, giving rise to a chain of alternating U(1) and U(2) bipyramids that is one polyhedron wide, and that extends along [10−1]. The arsenate tetrahedra are attached to either side of the chains by sharing edges with uranyl polyhedra (Fig. 5), and equatorial vertices with uranyl polyhedra from adjacent chains, resulting in sheets that are parallel to (010). The orientations of the tetrahedra alternate along the length of any chain such that the apical (non-sheet) tetrahedral ligand occurs alternately above and below the sheet. This arrangement is the

Table 7
Selected interatomic distances (Å) and angles (deg) for *PiperUP*

U(1)–O(6)	1.751(9)	U(4)–O(12)	1.74(1)	P(3)–O(24)	1.483(8)
U(1)–O(17)	1.754(9)	U(4)–O(16)	1.748(9)	P(3)–O(15)	1.501(8)
U(1)–O(11)	2.317(9)	U(4)–O(8)	2.302(8)	P(3)–O(21)	1.549(7)
U(1)–O(1)	2.381(7)	U(4)–O(3)	2.342(9)	P(3)–O(1)	1.555(8)
U(1)–O(21)	2.392(7)	U(4)–O(10)	2.355(7)	⟨P(3)–O⟩	1.52
U(1)–O(19)	2.469(7)	U(4)–O(7)	2.499(7)		
U(1)–O(2)	2.505(8)	U(4)–O(4)	2.513(8)	P(4)–O(20)	1.489(8)
⟨U(1)–O_{ap}⟩	1.75	⟨U(4)–O_{ap}⟩	1.74	P(4)–O(11)	1.546(9)
⟨U(1)–O_{eq}⟩	2.41	⟨U(4)–O_{eq}⟩	2.40	P(4)–O(2)	1.552(8)
O(6)–U(1)–O(17)	178.2(4)	O(12)–U(4)–O(16)	178.1(4)	P(4)–O(19)	1.556(8)
				⟨P(4)–O⟩	1.54
U(2)–O(22)	1.736(9)	U(5)–O(26)	1.750(7)		
U(2)–O(13)	1.76(1)	U(5)–O(25)	1.764(8)	N(1)–C(4)	1.43(2)
U(2)–O(15)	2.307(8)	U(5)–O(20)	2.335(8)	N(1)–C(1)	1.47(2)
U(2)–O(19)	2.351(7)	U(5)–O(18)	2.349(8)		
U(2)–O(2)	2.353(8)	U(5)–O(23)	2.388(7)	N(2)–C(2)	1.47(2)
U(2)–O(1)	2.489(7)	U(5)–O(24)	2.389(7)	N(2)–C(3)	1.49(2)
U(2)–O(21)	2.497(7)	U(5)–O(27)	2.551(9)		
⟨U(2)–O_{ap}⟩	1.75	⟨U(5)–O_{ap}⟩	1.76	C(1)–C(3)	1.48(2)
⟨U(2)–O_{eq}⟩	2.40	⟨U(5)–O_{eq}⟩	2.40	C(2)–C(4)	1.55(1)
O(22)–U(2)–O(13)	178.8(4)	O(26)–U(5)–O(25)	179.6(4)		
				OW(1)–N(2)	3.11(4)
U(3)–O(5)	1.753(9)	P(1)–O(23)	1.488(8)	OW(1)–O(12)	3.17(4)
U(3)–O(14)	1.760(9)	P(1)–O(8)	1.523(9)		
U(3)–O(9)	2.291(7)	P(1)–O(7)	1.563(8)	OW(2)–O(27)	2.83(3)
U(3)–O(4)	2.369(8)	P(1)–O(4)	1.568(8)	OW(2)–O(15)	3.10(4)
U(3)–O(7)	2.394(7)	⟨P(1)–O⟩	1.54		
U(3)–O(10)	2.480(7)				
U(3)–O(3)	2.522(8)	P(2)–O(18)	1.490(9)		
⟨U(3)–O_{ap}⟩	1.76	P(2)–O(3)	1.543(9)		
⟨U(3)–O_{eq}⟩	2.41	P(2)–O(10)	1.556(7)		
O(5)–U(3)–O(14)	176.6(3)	P(2)–O(9)	1.562(8)		
		⟨P(2)–O⟩	1.54		

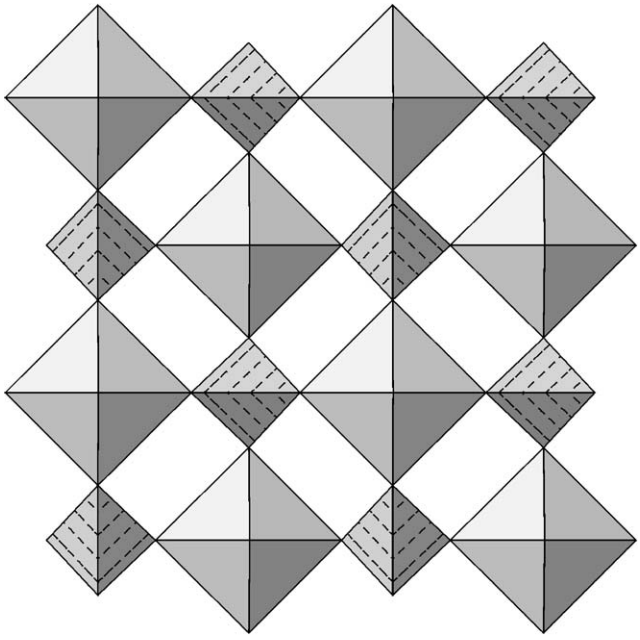

Fig. 1. The autunite-type uranyl arsenate sheet found in *DabcoUAs*, projected onto (010). The uranyl polyhedra are shown in shades of gray and the arsenate tetrahedra are stippled.

aa|aa geometrical isomer of the uranophane sheet-anion topology [46].

There are two symmetrically independent As atoms in *TriethUAs*, both of which are in distorted tetrahedral coordination (Table 6). As(1) is the center of an AsO_3OH group; the apical (non-sheet) ligand of the tetrahedron, O(12), has the longest distance to As(1), and with H(1), comprises a hydroxyl group (Table 6). As(2) is the center of an AsO_4 group; the apical ligand, O(8), has the shortest distance to As(2), and accepts hydrogen bonds from H(1) and H(2).

The triethylammonium cation in *TriethUAs* is located in the interlayer between the uranyl arsenate sheets (Fig. 6). The C(5)–C(6) ethyl group of this cation is disordered. During least-squares refinement, the C(5)–C(6) bond length refined to an unreasonably short distance, ~1.37 Å, and the displacement parameters of both atoms were larger than expected. The disorder was modeled with split positions (Table 3), yielding two half-occupied ethyl groups, C(5A)–C(6A) and C(5B)–C(6B) whose orientation is reminiscent of a pair of crossed arms (Fig. 7). It is likely that similar disorder is present in the phosphate isostructure, $\{NH(C_2H_5)_3\}[(UO_2)_2(PO_4)(PO_3OH)]$, despite data collection having been undertaken at 150 K. The

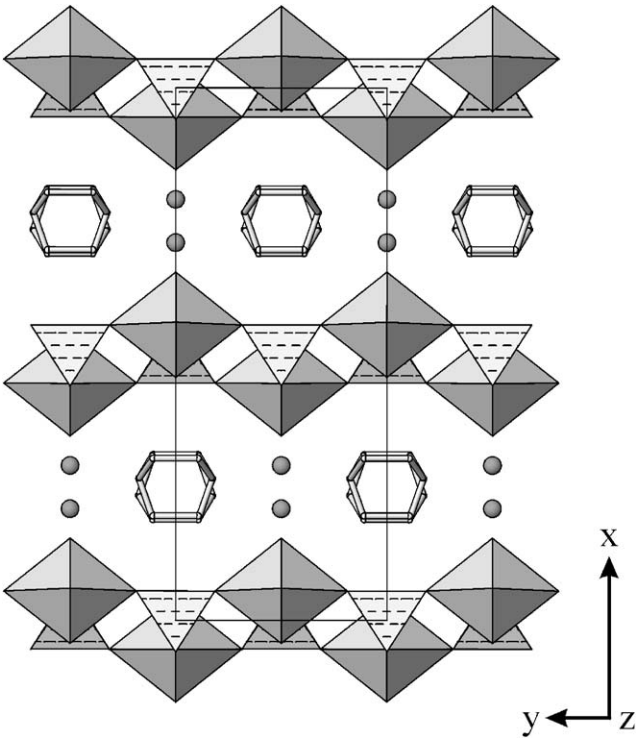

Fig. 2. The structure of *DabcoUAs* projected along [001]. The triethylenediammonium cations are represented as rods, and OW(1) as small spheres. OW(2A) is omitted for clarity.

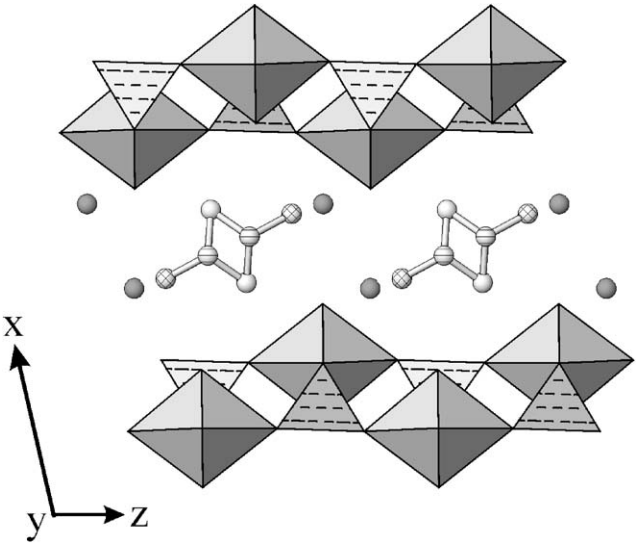

Fig. 3. Part of the structure of *DabcoUAs* projected along [010], showing the orientation and disorder of the triethylenediammonium cations and H_2O groups. N(1A) is shown as striped spheres, and is half-occupied, separated from its symmetry equivalent by 1.39(2) Å. C(2A) is shown as cross-hatched spheres and OW(2A) is shown as dark gray spheres; these positions are half-occupied and separated from each other by 1.27(1) Å. C(1) is fully occupied and shown as light gray spheres. OW(1) is omitted for clarity.

reported C(5)–C(6) bond length in this compound [16] is 1.24 Å, inconsistent with the presence of a single bond [47].

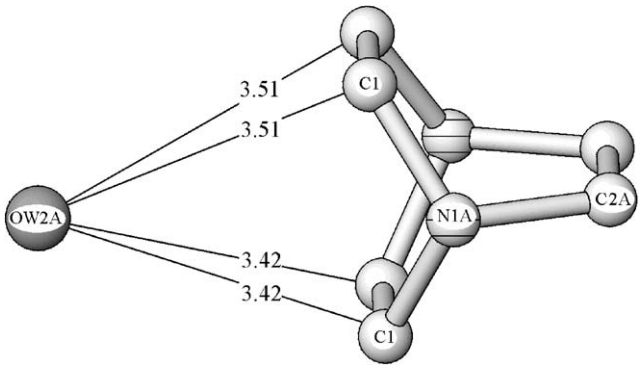

Fig. 4. The local environment of the triethylenediammonium cation. The separation distance from OW(2A) is 3.4–3.5 Å.

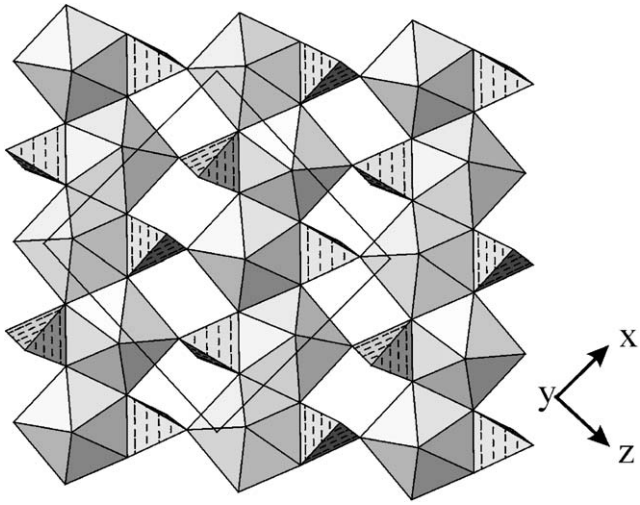

Fig. 5. The uranophane-beta type uranyl arsenate sheet in the structure of *TriethUAs*, projected along [010]. Tetrahedra on both sides of the uranyl chains alternate orientations along the chain length, giving rise to the geometrical isomer designation aa|aa. The uranyl polyhedra are shown in shades of gray and the arsenate tetrahedra are stippled.

The structure of *PiperUP* is also based on the aa|aa geometrical isomer of the uranophane sheet-anion topology. The uranyl phosphate sheet in *PiperUP* is topologically identical to the uranyl arsenate sheet in *TriethUAs*, and is oriented similarly with the sheet parallel to (010) and the direction of chain propagation along [10−1], but contains four symmetrically independent U atoms and four P atoms. The U(5) pentagonal bipyramid is located in the interlayer, between the uranyl phosphate sheets. Four equatorial oxygen atoms of the U(5) pentagonal bipyramid are shared with phosphate tetrahedra, providing linkage of the sheets, and resulting in an open uranyl phosphate framework structure (Fig. 8). The coordination polyhedron about U(5) is completed by an H_2O group—O(27). The

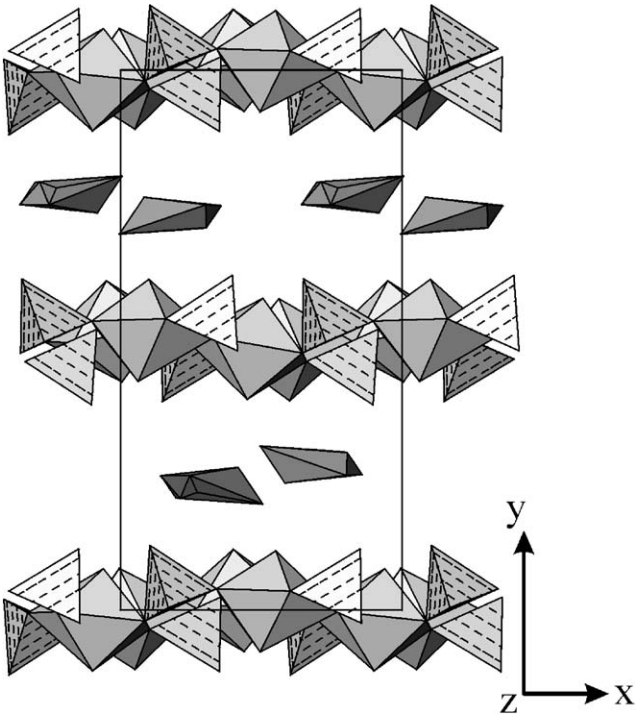

Fig. 6. The structure of *TriethUAs* projected along [001]. The triethylammonium cations are represented as isolated irregular polyhedra between the uranyl arsenate sheets.

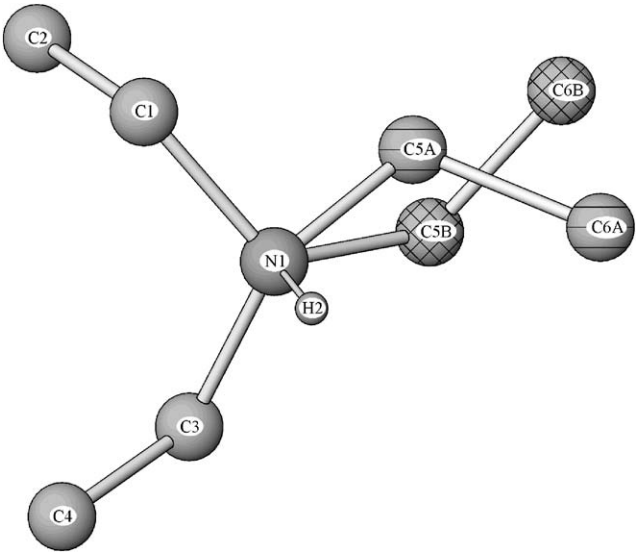

Fig. 7. Ball and stick representation of the triethylammonium cation in *TriethUAs*, showing the "crossed arm" disorder of the half-occupied C(5A)–C(6A) and C(5B)–C(6B) ethyl groups.

piperazinium cation occupies the large cavities in the framework (Fig. 8) along with two half-occupied H_2O groups—OW(1) and OW(2)—that are held in the structure only by hydrogen bonding.

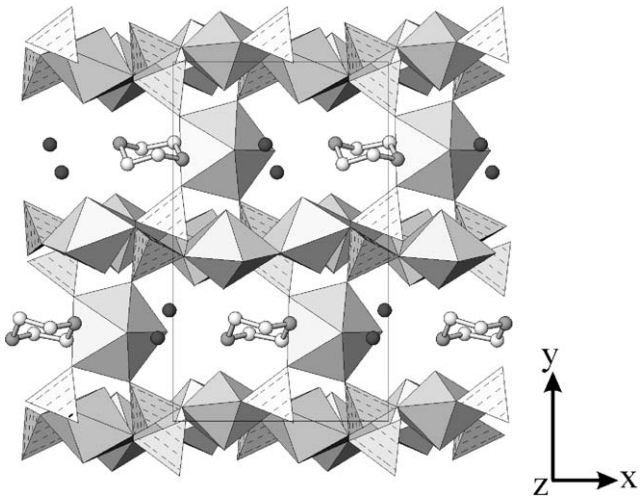

Fig. 8. The structure of *PiperUP* projected along [001]. The piperazinium cations occupy the large cavities of the structure. Carbon atoms are shown as light gray spheres and nitrogen atoms as medium gray spheres. The interstitial H_2O groups, OW(1) and OW(2), are half-occupied and separated from each other by 2.15(5) Å, and are shown as dark gray spheres. The uranyl polyhedra are shown in shades of gray and the arsenate tetrahedra are stippled.

4.2. Bond valence analysis

Bond valence analysis was performed using the coordination-specific parameters of Burns et al. [48] for U^{6+}, and the parameters of Brown and Altermatt [49] for As and P. For *DabcoUAs*, the bond valence sum at the U(1) site is 6.16 valence units (vu) and the sum at the As(1) site is 5.13 vu, consistent with formal valences of U^{6+} and As^{5+}. The bond valence sums for O(1) to O(5) range from 1.61 to 2.01 vu, consistent with their assignment as O atoms.

For *TriethUAs*, the bond valence sums at the U sites are 5.93 and 5.96 vu for U(1) and U(2), respectively, whereas the sums at the As sites are 5.12 and 5.03 vu for As(1) and As(2), respectively, consistent with formal valences of U^{6+} and As^{5+}. The bond valence sum for O(12) is 1.23 vu, consistent with its assignment as an hydroxyl group, whereas the bond valence sum for O(8) is rather low at 1.37 vu. If the hydrogen bonds from H(1) and H(2) to O(8) are included into the calculation [50], then the bond valence sum for O(8) increases to 1.83 vu, an acceptable value for an O atom. The bond valence sums for the remaining O atoms range from 1.71 to 2.18 vu.

For *PiperUP*, the bond valence sums at the U sites are 6.00, 6.11, 5.99, 6.13, and 6.03 vu for U(1)–U(5), respectively, and the sums at the P sites are 5.01, 4.97, 5.19 and 5.00 vu for P(1) to P(4), respectively, consistent with formal valences of U^{6+} and P^{5+}. The bond valence sum for O(27) is 0.37 vu, consistent with its assignment as an H_2O group. The bond valence sums for the O(1)–O(26) atoms range from 1.73 to 2.17 vu.

5. Discussion

5.1. Autunite-type sheets

Layered compounds containing the autunite-type sheet have long been known for their ion exchange properties [51]. A wide variety of inorganic cations can be intercalated between the negatively charged uranyl phosphate or uranyl arsenate sheets, including alkali metals, alkaline earths, transition metals, aluminum, and lanthanides, as well as complex ions such as oxonium, ammonium and metal-amine complexes [51–63].

Organic cations, generally protonated amines, have also been intercalated between autunite-type sheets [64,65], with recent attention focused on the intercalation and post-intercalative polymerization of aniline [66–70], and the intercalation of polyamine metal complexes [71]. Until now, no crystal structures of amine-bearing autunite-type compounds have been reported, possibly because the intercalation process does not yield single crystals; the expansion or contraction of interlayer space during the exchange process induces disorder and the resultant mosaic spread is more consistent with a powder sample [72,73]. *DabcoUAs* is apparently the first organic-bearing autunite-type structure to be refined. It is probable that synthesis using mild hydrothermal conditions would yield further well-crystallized examples of this structure type, and permit a more detailed understanding of the configurations of the organic guest molecules between the sheets.

5.2. Uranophane topology

The uranophane sheet-anion topology is adapted by a wide variety of minerals and inorganic uranyl compounds, including silicates, phosphates, arsenates and vanadates (reviewed in Ref. [46]). Geometrical variability within the uranophane type-sheet is generally limited to changes in the orientation of the tetrahedra, for which six geometrical isomers have been recognized [46], but the sheet does not have to remain planar, and puckered [16] or even highly corrugated examples have been described [46]. Extension of the chemical system to phosphonates reveals similar themes in structures based on the uranophane-type sheet: a uranyl methylphosphonate has the aa|aa geometrical isomer [18], whereas a uranyl chloromethylphosphonate shows the du|du isomer [21]. One of the uranyl phenylphosphonate compounds is unique in that the uu|uu isomer of the uranophane sheet has been curved to form tubes of finite width and infinite length, rather than infinite sheets [22].

In addition to sheet structures, inorganic framework structures are observed, in which interlayer uranyl polyhedra share equatorial vertices with the tetrahedra of the uranophane-type sheet, thereby providing linkage in the third dimension [9,46,74–76]. The cavities in these frameworks are occupied by H_2O groups and low-valence cations.

The use of amines as structure-directing agents in the synthesis of uranyl phosphates and uranyl arsenates can lead both to uranophane-type sheet structures (triethylamine, tetrapropylamine [16, this work]) and framework structures (diethylamine, piperazine [8, this work]) analogous to those of inorganic uranyl phosphates and uranyl arsenates. The exact role of the organic cations in the formation of extended structures has remained elusive [77], beyond their charge-balancing and space-filling roles. Careful control of hydrothermal reaction conditions in the piperazine–uranyl–phosphonate system has demonstrated that structural diversity is a function of reactant concentrations [26], consistent with the concept of a structure-directing agent, rather than a template sensu stricto [78].

Acknowledgments

This research was supported by the Environmental Management Science Program of the Office of Science, US Department of Energy, grants DE-FGO7-97ER14820 and DE-FGO7-02ER63489. We thank Sergey Krivovichev for encouraging this work. AJL thanks the Environmental Molecular Sciences Institute, University of Notre Dame, for a 2003 EMSI Fellowship, and the International Centre for Diffraction Data for a 2004 Ludo Frevel Crystallography Scholarship.

References

[1] P.C. Burns, M.L. Miller, R.C. Ewing, Can. Mineral. 34 (1996) 845–880.
[2] F. Demartin, C.M. Gramaccioli, T. Pilati, Acta Crystallogr. C 48 (1992) 1–4.
[3] J.M. Jackson, P.C. Burns, Can. Mineralogist 39 (2001) 187–195.
[4] Y. Li, P.C. Burns, J. Nucl. Mater. 299 (2001) 219–226.
[5] S.V. Krivovichev, C.L. Cahill, P.C. Burns, Inorg. Chem. 41 (2002) 34–39.
[6] S.V. Krivovichev, P.C. Burns, Can. Mineralogist. 39 (2001) 207–214.
[7] M. Saadi, C. Dion, F. Abraham, J. Solid State Chem. 150 (2000) 72–80.
[8] J.A. Danis, W.H. Runde, B. Scott, J. Fettinger, B. Eichhorn, Chem. Commun. 22 (2001) 2378–2379.
[9] A.J. Locock, P.C. Burns, J. Solid State Chem. 163 (2002) 275–280.
[10] P.S. Halasyamani, R.J. Francis, S.M. Walker, D. O'Hare, Inorg. Chem. 38 (1999) 271–279.
[11] S.M. Walker, P.S. Halasyamani, S. Allen, D. O'Hare, J. Am. Chem. Soc. 121 (1999) 10513–10521.
[12] S. Allen, S. Barlow, P.S. Halasyamani, J.F.W. Mosselmanns, D. O'Hare, S.M. Walker, R.I. Walton, Inorg. Chem. 39 (2000) 3791–3798.
[13] J.A. Danis, M.R. Lin, B.L. Scott, B.W. Eichhorn, W.H. Runde, Inorg. Chem. 40 (2001) 3389–3394.
[14] C.L. Cahill, P.C. Burns, Inorg. Chem. 40 (2001) 1347–1351.

[15] S.V. Krivovichev, P.C. Burns, J. Solid State Chem. 170 (2003) 106–117.
[16] R.J. Francis, M.J. Drewitt, P.S. Halasyamani, C. Ranganathachar, D. O'Hare, W. Clegg, S.J. Teat, Chem. Commun. (1998) 279–280.
[17] J.A. Danis, H.T. Hawkins, B.L. Scott, W.H. Runde, B.E. Scheetz, B.W. Eichhorn, Polyhedron 19 (2000) 1551–1557.
[18] D. Grohol, F. Gingl, A. Clearfield, Inorg. Chem. 38 (1999) 751–756.
[19] D. Grohol, M.A. Subramanian, D.M. Poojary, A. Clearfield, Inorg. Chem. 35 (1996) 5264–5271.
[20] D. Grohol, A. Clearfield, J. Am. Chem. Soc. 119 (1997) 4662–4668.
[21] D.M. Poojary, D. Grohol, A. Clearfield, J. Phys. Chem. Solids 56 (1995) 1383–1388.
[22] D.M. Poojary, D. Grohol, A. Clearfield, Angew. Chem. Int. Ed. Engl. 34 (1995) 1508–1510.
[23] D.M. Poojary, A. Cabeza, M.A.G. Aranda, S. Bruque, A. Clearfield, Inorg. Chem. 35 (1996) 1468–1473.
[24] D. Grohol, A. Clearfield, J. Am. Chem. Soc. 119 (1997) 9301–9302.
[25] M.A.G. Aranda, A. Cabeza, S. Bruque, D.M. Poojary, A. Clearfield, Inorg. Chem. 37 (1998) 1827–1832.
[26] M.B. Doran, A.J. Norquist, D. O'Hare, Chem. Mater. 15 (2003) 1449–1455.
[27] M. Doran, S.M. Walker, D. O'Hare, Chem. Commun. 19 (2001) 1988–1989.
[28] M.B. Doran, C.L. Stuart, A.J. Norquist, D. O'Hare, Chem. Mater. 16 (2004) 565–566.
[29] R. Mercier, M. Pham Thi, Ph. Colomban, Solid State Ionics 15 (1983) 113–126.
[30] T.M. Gesing, C.H. Rüscher, Z. Anorg. Allg. Chem. 626 (2000) 1414–1420.
[31] K. Mereiter, Tschermaks Mineral. Petrog. Mitt. 30 (1982) 129–139.
[32] W. Krause, H. Effenberger, F. Brandstätter, Eur. J. Mineral. 7 (1995) 1313–1324.
[33] H.F. Walton, Inorganic Preparations, A Laboratory Manual. Prentice-Hall Inc., New York, 1948, pp. 143–144.
[34] W.H. Dennis Jr., L.A. Hull, D.H. Rosenblatt, J. Org. Chem. 32 (1967) 3783–3787.
[35] SMART, Bruker AXS, Madison, WI, 1998.
[36] SAINT, Bruker AXS, Madison, WI, 1998.
[37] XPREP, Bruker AXS, Madison, WI, 1998.
[38] A.J.C. Wilson (Ed.), International Tables for X-ray Crystallography, Vol. C, Kluwer Academic Press, Boston, 1992.
[39] G.M. Sheldrick, SHELXTL Version 6.10, Bruker AXS, Madison, WI, 2000.
[40] Y. LePage, J. Appl. Crystallogr. 20 (1987) 264–269.
[41] A.L. Spek, J. Appl. Crystallogr. 36 (2003) 7–13.
[42] J. Beintema, Recl. Trav. Chim. Pays-Bas 57 (1938) 155–175.
[43] R.E. Marsh, Acta Crystallogr. B 51 (1995) 897–907.
[44] P.C. Burns, Can. Mineral. 36 (1998) 847–853.
[45] K. Viswanathan, O. Harneit, Am. Mineral. 71 (1986) 1489–1493.
[46] A.J. Locock, P.C. Burns, J. Solid State Chem. 176 (2003) 18–26.
[47] F.H. Allen, O. Kennard, D.G. Watson, L. Brammer, A.G. Orpen, R. Taylor, J. Chem. Soc. Perkin Trans. II (1987) S1–S19.
[48] P.C. Burns, R.C. Ewing, F.C. Hawthorne, Can. Mineral. 35 (1997) 1551–1570.
[49] I.D. Brown, D. Altermatt, Acta Crystallogr. B 41 (1985) 244–247.
[50] G. Ferraris, G. Ivaldi, Acta Crystallogr. B 40 (1984) 1–6.
[51] J.G. Fairchild, Am. Mineral. 14 (1929) 265–275.
[52] E. Schlute, Neues Jahrb. Mineral. Monatsh. (1965) 242–246.
[53] K. Walenta, Chem. Erde 24 (1965) 254–278.
[54] F. Weigel, G. Hoffmann, J. Less Common Met. 44 (1976) 99–123.
[55] R. Pozas-Tormo, L. Moreno-Real, M. Martínez-Lara, S. Bruque-Gamez, Can. J. Chem. 64 (1986) 30–34.
[56] R. Pozas-Tormo, L. Moreno-Real, M. Martínez-Lara, E. Rodríguez-Castellón, Can. J. Chem. 64 (1986) 35–39.
[57] R. Pozas-Tormo, L. Moreno-Real, M. Martínez-Lara, S. Bruque-Gamez, Inorg. Chem. 26 (1987) 1442–1445.
[58] G.L. Rosenthal, A.B. Ellis, J. Less Common Met. 139 (1988) 299–304.
[59] P.K. Dorhout, D.M. Sabel, A.B. Ellis, M. Martínez-Lara, S. Bruque-Gamez, J.L. Sanchez-Reina, L. Moreno-Real, J. Less Common Met. 156 (1989) 439–449.
[60] N.G. Chernorukov, E.V. Suleimanov, S.V. Barch, E.V. Alekseev, Radiochemistry (Transl. of Radiokhimiya) 43 (2001) 233–241.
[61] N.G. Chernorukov, N.V. Karyakin, E.V. Suleimanov, G.N. Chernorukov, Radiochemistry (Transl. of Radiokhimiya) 36 (1994) 227–232.
[62] N.G. Chernorukov, N.V. Karyakin, E.V. Suleimanov, G.N. Chernorukov, Russ. J. Inorg. Chem. (Transl. of Zh. Neorg. Khim.) 39 (1994) 20–23.
[63] R.V. Gaines, H.C.W. Skinner, E.E. Foord, B. Mason, A. Rosenzweig, V.T. King, Dana's New Mineralogy, 8th Edition. Wiley, New York, NY, 1997, 1819pp.
[64] A. Weiss, K. Hartl, U. Hofmann, Z. Naturforsch. B: Anorg. Chem. Org. Chem. Biochem. Biophys. Biol. 12b (1957) 351–355.
[65] M. Fernández-González, A. Weiss, K. Beneke, G. Lagaly, Z. Naturforsch. B: Anorg. Chem. Org. Chem. Biochem. Biophys. Biol. 31b (1976) 1205–1211.
[66] L. Moreno-Real, R. Pozas-Tormo, M. Martínez-Lara, S. Bruque, Mater. Res. Bull. 22 (1987) 19–27.
[67] M. Martínez-Lara, J.A. Barea-Aranda, L. Moreno-Real, S. Bruque, J. Inclusion Phenom. Mol. Recognit. Chem. 9 (1990) 287–299.
[68] Y.-J. Liu, M.G. Kanatzidis, Inorg. Chem. 32 (1993) 2989–2991.
[69] Ph. Colomban, A. Efremova, A. Gruger, A. Novak, Solid State Ionics 78 (1995) 19–30.
[70] Y.-J. Liu, M.G. Kanatzidis, Chem. Mater. 7 (1995) 1525–1533.
[71] D. Grohol, E.L. Blinn, Inorg. Chem. 36 (1997) 3422–3428.
[72] G. Alberti, U. Constantino, Compr. Supramol. Chem. 7 (1996) 1–24.
[73] A. Clearfield, U. Constantino, Compr. Supramol. Chem. 7 (1996) 107–150.
[74] A.J. Locock, P.C. Burns, J. Solid State Chem. 167 (2002) 226–236.
[75] A.J. Locock, P.C. Burns, J. Solid State Chem. 175 (2003) 372–379.
[76] A.J. Locock, P.C. Burns, Z. Kristallogr., 2004, in press.
[77] A.C. Bean, T.E. Albrecht-Schmitt, J. Solid State Chem. 161 (2001) 416–423.
[78] M.E. Davis, R.F. Lobo, Chem. Mater. 4 (1992) 756–768.